Retarded Interactions in Fermi Systems. II. Quasiparticle Lifetimes

C. B. DOVER* AND R. H. LEMMER†

Physics Division, South African Atomic Energy Board, Pelindaba, Pretoria, Republic of South Africa

(Received 10 September 1968)

Properties of the inverse lifetime $1/\tau$ of quasiparticles in an infinite system of nucleons ("nuclear matter") interacting via the exchange of a neutral scalar boson are studied in the dielectric formulation of the many-body problem. It is shown that the polarization of the nuclear medium plays an essential role in determining $1/\tau$. The presence of the medium mediates the interaction between two nucleons in it through the introduction of an effective "dielectric constant" for nuclear matter. The interaction becomes "dressed" in a fashion analogous to, but different in its details from, the screening of the Coulomb interaction between electrons in metals. Calculations of $1/\tau$ are made for nuclear matter both in second-order perturbation theory, and using the fully dressed interaction calculated in the random-phase approximation (RPA). The RPA estimate is lower by about a factor of 3 over a wide range of momenta and is in good agreement with empirical optical-model estimates of $1/\tau$. The second-order perturbation estimate is by contrast *entirely* inadequate, emphasizing the importance of taking the polarization effects into account for scattering processes at actual nuclear densities. The use of a dielectric constant for the medium also introduces another feature into the properties of $1/\tau$. The behavior of $1/\tau$ near the Fermi surface now becomes sensitive to whether or not the interacting ground state is unstable with respect to a permanent density fluctuation. If it is, then $1/\tau$ behaves like $(p-p_F)$ instead of $(p-p_F)^2$ near the Fermi surface (p_F is the Fermi momentum). This is *not* a new physical result, but rather a reflection of the inadequacy of the RPA if the system becomes unstable. It is shown that as the momentum increases the effect of such an instability, if present, decreases, and becomes entirely negligible when $p \gtrsim \sqrt{2} p_F$.

I. INTRODUCTION

In a previous article,[1] some properties of a system of fermions interacting via the exchange of a massive boson were considered. Such a system is reminiscent of nucleons in nuclear matter interacting via the exchange of the various mesons that are thought to provide the nucleon-nucleon interaction. Of course, restricting the exchange to one type of boson only is quite unrealistic. At most we can hope to study the effects of the long-range part of nuclear forces in nuclear matter [one-pion-exchange potential (OPEP)] in such a model by identifying the exchanged particle with a pion. Indeed, the expected feature of the complete collapse in the ground state of such a system was demonstrated in I. This difficulty is directly related to the lack of a repulsive component in the effective interaction. However, some properties of such a model system are expected to be less sensitive to the instability problem of the ground state as far as their qualitative behavior is concerned. In particular, the Hartree-Fock field of the system is one such property.[1] We calculated this field in I, using nucleons interacting by exchange of either one neutral scalar or a triplet of pseudoscalar bosons as an illustration of the model. It was shown there that the main effect of explicitly introducing the boson exchange between nucleons is to produce a frequency-dependent interaction (i.e., an interaction that is not instantaneous in time) between nucleons. However, the effects of such a frequency dependence are essentially controlled by the ratio of nucleon kinetic energy to boson rest mass μ and therefore only show up at energies $\sim\mu$. If the exchanged particle has a mass of a pion ($\mu\approx 135$ MeV), this is a relatively high energy for a nucleon in a nucleus.

In analogy with the state of affairs in an interacting electron gas,[2] the interaction between nucleons in nuclear matter is expected to become "dressed" owing to the excitation of virtual particle-hole pairs out of the Fermi sea. This process leads to the usual polarization cloud that converts a particle into a quasiparticle. Such quasiparticle states are, of course, not exact eigenstates of the interacting system; they have a finite lifetime τ, or width[3] $1/\tau = -2\,\mathrm{Im}\Sigma(\mathbf{p})$ representing their decay into more complicated excitations. Here, $\Sigma(\mathbf{p})$ is the self-energy of a quasiparticle of momentum $\mathbf{p}$. An estimate of $1/\tau$ is interesting for several reasons: (i) The quasiparticle concept has a well-defined meaning only if $\epsilon_p \tau \gg 1$, where ϵ_p is the excitation energy; this condition is density-dependent through the dependence of τ on density (through the Fermi momentum p_F). It is therefore of interest to investigate the range of particle energies ϵ_p for which the quasiparticle picture holds for the present model at actual nuclear densities. (ii) The width of quasiparticle excitations in real nuclei can be identified with the magnitude of the absorptive part of the optical potential. This is known empirically for nucleon-nucleus scattering over a wide range of energies[4,5] so that a direct contact with experiment is

*Winter visitor, on leave from the Institut für Theoretische Physik der Universität Heidelberg, Heidelberg, West Germany.

†Visiting research leader from Physics Department, UNISA, Pretoria.

[1] C. B. Dover and R. H. Lemmer, Phy. Rev. **165**, 1105 (1968). This paper will be referred to as I.

[2] K. Sawada, Phys. Rev. **106**, 372 (1957); K. Sawada, K. A. Brueckner, N. Fukuda, and R. Brout, *ibid.* **108**, 507 (1957).

[3] Units $\hbar = c = 1$ are used throughout.

[4] F. Bjorklund, in *Proceedings of the International Conference on the Nuclear Optical Model, Florida State University Studies, No. 32*, edited by A. E. S. Green, C. E. Porter, and D. S. Saxon (The Florida University Press, Tallahassee, Florida, 1959), p. 1.

[5] C. A. Engelbrecht and H. Fiedeldey, Ann. Phys. (N.Y.) **42**, 262 (1967).

possible. (iii) Estimates of $1/\tau$ for real nuclear systems have been essentially restricted to the use of second-order perturbation theory owing to the complexity of such systems.[6] However, in nuclear matter one is able to go beyond the perturbation calculation result by summing over a restricted class of interaction diagrams (polarization or "bubble" diagrams) that describe the "dressing" process due to the polarization of the medium,[7] and give rise to a modified interaction between nucleons.

The modified, or "dressed" interaction for nucleons exchanging neutral scalar bosons is calculated in Sec. II. It is shown that the dressing process leads to an interaction of longer range and weaker strength than the original one, in contrast to what is found in the electron gas.[7] The difference arises because of the attractive nature of the nuclear interaction in the present model. The inverse lifetime $1/\tau$ is calculated in Sec. III using (a) perturbation theory and (b) the fully dressed interaction. It is shown that, while the perturbation calculation always gives the expected $(p-p_F)^2$ dependence of $1/\tau$ on momentum near the Fermi surface, this is not necessarily true for the dressed interaction. If the ground state is unstable against a permanent density fluctuation (this always happens in the present model[1] if the nucleon-boson coupling is strong enough), an "instability pole" is present in the dressed interaction at low incident momentum that forces $1/\tau$ to behave like $(p-p_F)$ near the Fermi surface. At higher momenta $(p\gtrsim\sqrt{2}p_F)$, this pole does not interfere and the calculation of $1/\tau$ is probably adequate. The calculation of inverse lifetime is carried out over a wide range of energies (momenta) and a comparison with experimental data is presented.

II. DRESSED INTERACTION

It was shown in I that the interaction between two nucleons has the form

$$V_k(\omega)=\lambda^2 D_k(\omega) \tag{1}$$

in a momentum-frequency representation, for the exchange of neutral scalar bosons, or

$$V_k(\omega)=(f/\mu)^2(\boldsymbol{\sigma}_1\cdot\mathbf{k})(\boldsymbol{\sigma}_2\cdot\mathbf{k})(\boldsymbol{\tau}_1\cdot\boldsymbol{\tau}_2)D_k(\omega) \tag{1'}$$

if a pseudoscalar boson is exchanged. In the latter expression $\boldsymbol{\sigma}$ and $\boldsymbol{\tau}$ refer to the spin and isospin operators of a single nucleon. Further,

$$D_k(\omega)=1/(\omega^2-\Omega_k^2) \tag{2}$$

is the propagator, or Green's function, for a boson of momentum $\mathbf{k}$ and energy Ω_k. We assume the relation $\Omega_k=(k^2+\mu^2)^{1/2}$, where μ is the rest mass; that is, the free-boson propagation is governed by a Klein-Gordon equation. Finally, λ and f are dimensionless coupling constants. The zero frequency limits of (1) and (1') just reduce to the form of nucleon-nucleon interaction given by a Yukawa-type[8] or Chew-Low-type[9] coupling between mesons and static nucleons, respectively.

Now while (1') is certainly more realistic [being the origin of the long-range one-pion exchange potential (OPEP) part of the nucleon-nucleon interaction], in general, it does not, by itself, allow the well-known dipole state[10] to exist in nuclear matter (see I). On the other hand, the interaction (1) does, and produces this state at the correct excitation energy for a value of the coupling constant λ ($\lambda^2=5$) that is known from shell-model calculations using Yukawa potentials with adjustable strengths. Therefore, in what follows we will calculate with the simpler form of interaction (1), since this will allow us to compare quasiparticle lifetimes of a system that possesses at least some properties expected of nuclear matter.

In I, the Hartree-Fock field generated by (1) was calculated; that is, we calculated the contribution to the self-energy $\Sigma(\mathbf{p})$ to first order in the interaction only, see Figs. 1(a) and 1(b). Higher-order contributions to $\Sigma(\mathbf{p})$ come from polarization processes of the Fermi vacuum like those shown in Fig. 1(c). It is well known[7] that the contribution from the infinite string of particle-hole pair excitations [represented as bubbles in Fig. 1(c)] can be summed in closed form to obtain an effective or "dressed" interaction,

$$V_k^{(d)}(\omega)=\frac{\lambda^2 D_k(\omega)}{1+g\lambda^2 D_k(\omega)\Pi_0(k,\omega)} \tag{3}$$

if the bare interaction is given by (1). Here, $\Pi_0(k,\omega)$ represents the polarization contribution of a "bubble" with momentum $\mathbf{k}$ and frequency ω:

$$\Pi_0(k,\omega)=\sum_{|\mathbf{p}+\mathbf{k}|>p_F>p} 2\omega^0{}_{\mathbf{pk}}/(\omega^{02}{}_{\mathbf{pk}}-\omega^2) \tag{4}$$

that is made up of all particle-hole pair excitations of energy $\omega^0{}_{\mathbf{pk}}=\epsilon_{\mathbf{p}+\mathbf{k}}-\epsilon_{\mathbf{p}}$ and momentum $\mathbf{k}$. The spin-isospin factor g ($g=4$ for nucleons) has not been included in our definition of $\Pi_0(k,\omega)$ contrary to the usual practice. By analogy with the electron gas case, the denominator in Eq. (3) defines a "dielectric constant" for nuclear matter. Since we have only included excitations of the Fermi vacuum of a special type (bubbles), the result (3) amounts to calculating the dielectric constant in the RPA. One writes

$$V_k^{(d)}(\omega)=\lambda^2 D_k(\omega)/\epsilon_{\mathrm{RPA}}(k,\omega),$$

$$\epsilon_{\mathrm{RPA}}(k,\omega)=1+g\lambda^2 D_k(\omega)\Pi_0(k,\omega). \tag{5}$$

[6] See, for example, K. A. Brueckner, Phys. Rev. **103**, 172 (1956); K. A. Brueckner, R. J. Eden, and N. C. Francis, *ibid.* **100**, 891 (1955); A. M. Lane and C. F. Wandel, *ibid.* **98**, 1524 (1955); M. Cini and S. Fubini, Nuovo Cimento **10**, 75 (1955).

[7] P. Nozières and D. Pines, *Quantum Theory of Liquids* (W. A. Benjamin, Inc., New York, 1966); R. D. Mattuck, *A Guide to Feynman Diagrams in the Many-Body Problem* (McGraw-Hill Book Co., New York, 1967).

[8] H. Yukawa, Proc. Phys. Math. Soc. Japan **17**, 48 (1935).

[9] G. F. Chew and F. E. Low, Phys. Rev. **101**, 1570 (1956).

[10] W. Brenig, Nucl. Phys. **22**, 14 (1961).

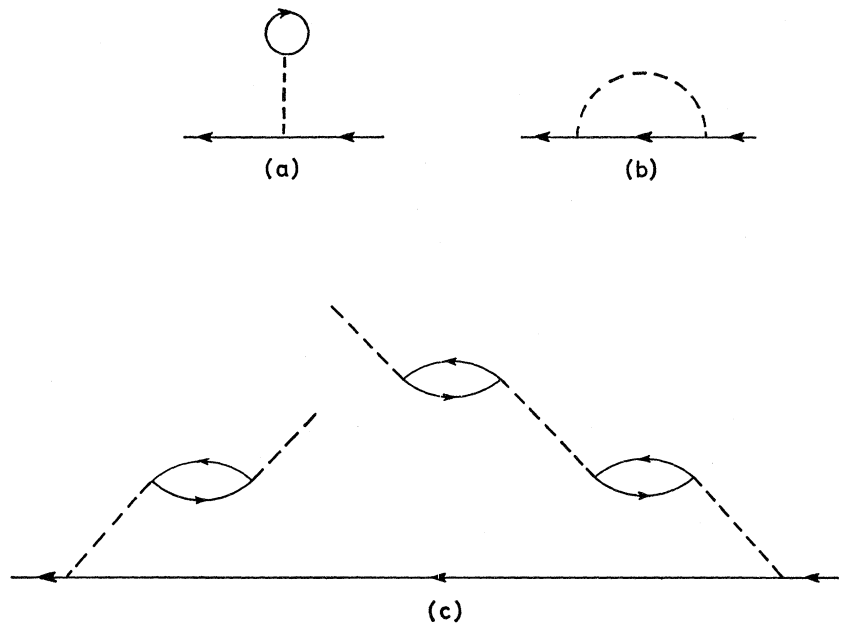

FIG. 1. Some interaction diagrams for the nucleon-boson system: (a) Hartree and (b) Hartree-Fock contribution to the self-energy of a nucleon (directed solid lines) exchanging a boson (dashed lines) with a background particle or itself. (c) Particle-hole excitations of the medium initiated by the incident nucleon coming into the diagram on the right. The reversed arrows indicate hole states in the Fermi sea.

The condition $\epsilon_{\mathrm{RPA}}(k,\omega)=0$ then defines a dispersion relation yielding the momenta and energies at which the system displays collective excitations.[7] We already discussed the question of collective excitations in the present model in I, where it was shown that (5) contains unstable excitations for certain ranges of momenta $\mathbf{k}$ and coupling constant $g\lambda^2$. These results will be important for our further discussion. An explicit expression for $\Pi_0(k,\omega)$ is available in the literature.[7,11] It is reproduced in Appendix A for convenience. In Appendix B, we discuss some analytic properties of $\epsilon_{\mathrm{RPA}}(k,\omega)$.

Let us consider some properties of the dressed interaction $V_k^{(d)}(\omega)$. At low frequencies, $\omega\ll\mu$ one has essentially the static result

$$V_k^{(d)}(\omega)\approx V_k^{(d)}(0)=-(\lambda^2/\Omega_k^2)[1/\epsilon_{\mathrm{RPA}}(k,0)] \quad (6)$$

or

$$V_k^{(d)}(0)=-\lambda^2/[\Omega_k^2-g\lambda^2\Pi_0(k,0)] \quad (7)$$

in more detail. Now for low momenta ($k\ll 2p_F$), the function $\Pi_0(k,0)$ possesses the simple expansion (this expansion is actually numerically acceptable for the entire range of k values up to about $2p_F$; see Fig. 3 in Appendix A)

$$(2\pi^2/mp_F)\Pi_0(k,0)\approx[1-\tfrac{1}{8}(k^2/p_F^2)]. \quad (8)$$

Substituting this result into Eq. (7) and regrouping, one finds that the dressed interaction is still of the Yukawa type with a modified strength and range:

$$V_k^{(d)}(0)=-\lambda_r^2/(\mu_r^2+k^2), \quad (9)$$

with

$$\lambda_r^2=\frac{\lambda^2}{1+g\lambda^2(m/16\pi^2p_F)}, \qquad \mu_r^2=\frac{\mu^2-g\lambda^2(mp_F/2\pi^2)}{1+g\lambda^2(m/16\pi^2p_F)}. \quad (10)$$

Note that $\lambda_r<\lambda$; the coupling strength is weakened by the action of the Fermi sea polarization processes. More significantly, the dressed interaction has a longer range $1/\mu_r>1/\mu$. In fact, if the coupling strength λ assumes the critical value

$$g\lambda^2=g\lambda_c^2=2\pi^2\mu^2/mp_F \quad (11)$$

for a given density (fixed p_F), the range becomes infinite. Larger values of $g\lambda^2$ give nonphysical values for μ_r^2 ($\mu_r^2<0$). This is not a real physical effect; rather it is an indication that the whole RPA method of calculation breaks down. For the value (11) of $g\lambda^2$ is precisely the threshold value of the coupling constant for a permanent density fluctuation (instability) to develop in the ground state of the system.[1] Negative values of μ_r^2, therefore, simply mean that the polarization effects "overcompensate" for such coupling constants, producing an unphysical situation within the confines of the RPA.

These properties are in contrast with the electron gas, where the bare Coulomb interaction $\sim 1/k^2$ becomes "screened" by the polarization processes to become $1/(k^2+k_{FT}^2)$, k_{FT}^{-1} being the Fermi-Thomas screening length or inverse mass of the exchanged phonon. The difference is due to the basic attractive nature of the long-range part of the nucleon-nucleon force as opposed to the repulsive Coulomb force between two electrons.

The situation is somewhat similar if we consider the

[11] D. Pines, *The Many-Body Problem* (W. A. Benjamin, Inc., New York, 1962).

"dynamic dressing" process at higher frequencies. Typically, we expect frequencies of interest to lie in the vicinity of the Fermi energy $\omega \sim \epsilon_F$ of the system, which is *large* in relation to the maximum particle-hole energy $\omega_k = kv_F$ in the long-wavelength limit, $k \to 0$ ($v_F = p_F/m$ is the velocity of a nucleon at the Fermi surface). Then [see Appendix A, Eq. (A12)] for $\omega \gg \omega_k$,

$$g\Pi_0(k,\omega) \approx -g(mp_F/6\pi^2)(\omega_k/\omega)^2 = -N(k^2/m\omega^2), \quad (12)$$

where N is the particle density. This means that again

$$V_k^{(d)}(\omega) \approx -\lambda_r^2/(\mu_r^2+k^2), \quad (13)$$

with

$$\lambda_r^2 = \frac{\lambda^2}{(1+N\lambda^2/m\omega^2)}, \qquad \mu_r^2 = \frac{\mu^2}{(1+N\lambda^2/m\omega^2)}, \quad (14)$$

but this result is now definitely restricted to long wavelengths. Notice that it is *not* possible to regain the static limit (10) by letting $\omega \to 0$ in Eq. (14); the $k \to 0$ and $\omega \to 0$ limiting procedures for the function $\Pi_0(k,\omega)$ do not commute. Qualitatively, we have the same conclusions as before; the coupling strength is weakened ($\lambda_r^2 < \lambda^2$), and the range is increased ($1/\mu_r > 1/\mu$). We notice in addition that the dressing becomes increasingly unimportant at high frequencies, $\lambda_r \to \lambda$ and $\mu_r \to \mu$ as $\omega \to \infty$, but becomes more effective as the particle density N increases.

III. SELF-ENERGY AND QUASIPARTICLE DAMPING

It is well known that the complete contribution to the self-energy $\Sigma(\mathbf{p})$ from bubble diagrams like those shown in Fig. 1(c) is obtained by simply replacing the free-boson line (dashed) in Fig. 1(b) representing the free propagator $D_k(\omega)$ by a "dressed" line representing the dressed propagator $D_k(\omega)\epsilon_{\mathrm{RPA}}^{-1}(k,\omega)$. The calculation, therefore, completely neglects the contribution of multiparticle excitations to $\Sigma(\mathbf{p})$. Quinn and Ferrell have already obtained the relevant formula for $\Sigma(\mathbf{p})$ using this approximation for the electron gas.[7,12] We merely quote their result for the imaginary part:

$$\tau^{-1} = -2\,\mathrm{Im}\Sigma(\mathbf{p}) = -2\sum_{\mathbf{k}}{}' \left[\lambda^2 D_k(\omega)\ \mathrm{Im}\epsilon_{\mathrm{RPA}}^{-1}(k,\omega)\right]_{\omega=\epsilon_{\mathbf{p}}-\epsilon_{\mathbf{p}-\mathbf{k}}}. \quad (15)$$

This formula must be evaluated subject to the following restrictions: (i) $\epsilon_{\mathrm{RPA}}(k,\omega)$ is now the causal dielectric constant that is obtained from Eq. (5) upon allowing ω to acquire a positive imaginary part, $\omega \to \omega + i\eta$, $\eta > 0$ in that expression.[7] (ii) The frequency ω in both $D_k(\omega)$ and $\epsilon_{\mathrm{RPA}}(k,\omega)$ must equal the energy difference $\epsilon_{\mathbf{p}} - \epsilon_{\mathbf{p}-\mathbf{k}}$ that a nucleon of energy $\epsilon_{\mathbf{p}}$ transfers to the system during a collision from momentum states $\mathbf{p}$ to $\mathbf{p}-\mathbf{k}$ that are both empty. (iii) This energy transfer must be positive. The last two conditions mean that

$$p^2 > |\mathbf{p}-\mathbf{k}|^2 > p_F^2, \quad (16)$$

which restricts the sum on $\mathbf{k}$ [the restriction is indicated by the prime on the summation sign in (15)], accordingly. It has been shown by Ritchie[13] that the result (15) is equivalent to calculating in second-order perturbation theory the total transition rate for particles of momentum $\mathbf{p}$ and energy $\epsilon_{\mathbf{p}}$, creating two-particle–one-hole states of the same total momentum and energy, via the dressed interaction (3).

A form for $1/\tau$ that is convenient for its numerical evaluation is given in Appendix C. However, for momenta near p_F only low frequencies $\omega = \epsilon_{\mathbf{p}} - \epsilon_{\mathbf{p}-\mathbf{k}} \ll \epsilon_F$ enter into (15), and one might as a first approximation ignore the frequency dependence in $|\epsilon_{\mathrm{RPA}}(k,\omega)|^2$ altogether. This amounts to using the form (9) for $V_k^{(d)}(0)$. Then the sum on $\mathbf{k}$ in (15) can be performed approximately, leading to the result

$$\tau^{-1} \approx \frac{3Nm}{8\pi}\left(\frac{p}{p_F}-1\right)^2 \int_0^{2p_F} dk \left(\frac{-\lambda_r^2}{\mu_r^2+k^2}\right)^2 = \frac{3Nm\lambda^4}{16\pi\mu_r^3}\left(\frac{p}{p_F}-1\right)^2\left[\frac{(2p_F/\mu_r)}{1+(2p_F/\mu_r)^2} + \tan^{-1}(2p_F/\mu_r)\right]. \quad (17)$$

Thus, $1/\tau$ displays the expected $(p-p_F)^2$ behavior near the Fermi surface.[7] There is one important remark, however: When the coupling strength $g\lambda^2$ reaches its critical value $g\lambda_c^2$ given in (11), this expression diverges. In fact, we shall show in Appendix D that the entire derivation leading to Eq. (17) becomes invalid when $\lambda \geq \lambda_c$. The presence of a permanent density fluctuation in the ground state then alters the behavior of the integrand in Eq. (15) in such a way as to make $1/\tau$ behave like $(p-p_F)$ instead of $(p-p_F)^2$ near the Fermi surface. This result is of course unphysical, but it is an interesting consequence of the instability of the ground state against a permanent density fluctuation. However, its effects are confined to momenta near p_F only. For larger values of p/p_F the instability problem has a negligible effect on the value of $1/\tau$.

IV. RESULTS AND DISCUSSION

It is not possible to carry out the integration over $\mathbf{k}$ analytically in Eq. (15) for all values of the momentum. We, therefore, have rewritten this equation in the form displayed as Eq. (C4) of Appendix C, which form is suitable for numerical integration. The value of $1/\tau$ obtained is shown in Fig. 2 as a function of p/p_F. For this calculation, we have taken the previously determined value of the coupling constant $\lambda^2 = 5$, that causes the dipole state in nuclear matter to lie at the correct

[12] J. J. Quinn and R. A. Ferrell, Phys. Rev. **112**, 812 (1958); see also A. S. Reiner, *ibid.* **129**, 889 (1963); **138**, B389 (1965).

[13] R. N. Ritchie, Phys. Rev. **114**, 644 (1959).

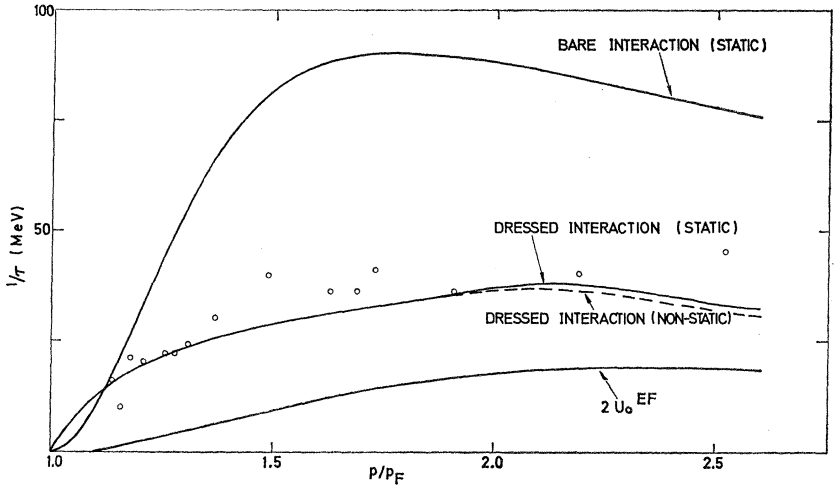

FIG. 2. Inverse lifetime for quasiparticle excitations. Three upper curves are labeled according to the interaction that was used to calculate them. The lower curve labeled $2U_0^{EF}$ gives the empirical estimate obtained from the optical-model parameters used in Ref. 5. The circles indicate older optical-model and/or theoretical estimates as given in Ref. 4.

excitation energy, in addition to assuming $\mu=135$ MeV for the exchanged boson, and $p_F=1.36$ fm^{-1} as a typical value for the Fermi momentum in nuclear matter.

We have also calculated the contribution to $1/\tau$ coming from a single "bubble" in the chain of Fig. 1(c), i.e., the second-order perturbation-theory result for $1/\tau$ using the bare interaction $\lambda^2 D_k(\omega)$ instead of the dressed one. If the static limit of the bare interaction is used, $\lambda^2 D_k(0)$, it is possible to obtain an analytic form for $1/\tau$ for all values of p/p_F. However, the result is too complicated to reproduce here and is therefore relegated to Appendix C. For p near p_F, however, this expression reduces to that given in Eq. (17) with μ_τ and λ_τ replaced by their "bare" values μ and λ. Using the values quoted above for μ, λ, and p_F, one has

$$(1/\tau)_{\text{bare}} \approx 1084[p/p_F-1]^2 \text{ MeV}$$

near the Fermi surface. The entire curve of $(1/\tau)_{\text{bare}}$ versus p/p_F as given by Eq. (C9) of Appendix C is also shown in Fig. 2.

A comparison of the two calculations of $1/\tau$ for the bare and dressed interaction shows the extreme importance of using the latter at actual nuclear densities. The effect of the polarization of the medium causes a reduction of $1/\tau$ of about a factor of 3 over most of the momentum range shown in Fig. 2. By contrast, the frequency dependence in $D_k(\omega)$ itself is not important. The difference between a dressed static and dressed nonstatic interaction is shown in Fig. 2, the dashed line indicating where the nonstatic interaction gives results that are distinguishable from the dressed static interaction. One also notes the expected $(p-p_F)^2$ behavior of $(1/\tau)_{\text{bare}}$ as opposed to the linear dependence of $1/\tau$ on momentum near the Fermi surface. We have already commented on the origin and unphysical nature of this difference. We show in Appendix D that the influence of the instability certainly becomes negligible when $p \geq \sqrt{2}\, p_F$.

Finally, Fig. 2 also shows some empirical values of $1/\tau$ as deduced from optical-model fitting of experimental data on nucleon-nucleus scattering. In order to compare our calculations with the quoted values of $1/\tau$, two assumptions are necessary: (i) $1/\tau$ as calculated in nuclear matter can be compared with the optical-model absorption strength in the interior of a real nucleus. This means we must only compare with the volume absorption part of the optical potential. Then $1/\tau = 2U_0$, where U_0 is the strength of the volume absorption part. (ii) Since scattering experiments only measure nuclear potentials at incident energies E_{inc} in excess of the binding energy of the incident particle to the target nucleus, we have to connect the energy ϵ_p of a nucleon with momentum $\mathbf{p}$ in nuclear matter to E_{inc} in some way. Assuming that the average binding energy of a nucleon in a real nucleus is 8 MeV and that $\epsilon_F=39$ MeV, for nuclear matter, one has the simple prescription that $\epsilon_p \approx \epsilon_F+8+E_{\text{inc}}$ or $p/p_F=[1+(8+E_{\text{inc}})/39]^{1/2}$. We have used this prescription in transferring empirical values of $1/\tau$ (which are given as a function of E_{inc}) to the momentum scale of Fig. 2.

The empirical data on $2U_0$ shown in Fig. 2 come from two sources. The circles show early ($\sim$1958) values of Bjorklund and Fernbach[4] found by optical-model fitting procedures and/or values of this quantity calculated according to the phase-shift prescription of Riesenfeld and Watson.[14] These values are to be contrasted with the recent extensive analysis[5] of neutron-nucleus scattering data by Engelbrecht and Fiedeldey, who find a considerably smaller value for the volume absorption strength (the curve marked $2U_0^{EF}$).

The calculated and empirical values of $1/\tau$ are seen to be in rather good agreement, especially as regards the older values from Ref. 4. However, in making this comparison one should always bear in mind that the calculated curves do not yet contain the contribution

[14] W. B. Riesenfeld and K. M. Watson, Phys. Rev. 102, 1157 (1956).

from multiparticle excitations that certainly must enter the picture also. One notes in particular that: (i) The shape of $1/\tau$ as a function of momentum is well reproduced[15]; (ii) the calculation using the bare interaction is *entirely* inadequate. This latter result suggests that the dressing processes are likely to also play an important role in real nuclei and require careful consideration in any attempt to calculate the optical potential for a finite system of nucleons. For example, within the framework of the shell model for nuclear structure.

The *qualitative* nature of these calculations should be reemphasized. We have only considered the exchange of a neutral scalar meson for illustrating the program in the present paper, and our results are phenomenological to this extent. The reason for this restriction has been discussed in Sec. II. More realistically, one would want to consider the exchange of pions, which are pseudoscalar. But then it becomes essential to also consider the exchange of heavier mesons such as ρ, ω, η at the very least, in order to reproduce the correct saturation properties for the ground state of "nuclear matter." This can be done relatively easily within the confines of the present model, and further investigations along these lines are planned. An indication that such calculations would be reasonable comes from the work of Bryan and Scott[16] on static, one-boson-exchange models for nucleon-nucleon forces. These authors show that the exchange of these heavier mesons generates a short-range repulsive component in the two-body force that is necessary to fit the two-body scattering phase shifts. Such a repulsive component in the effective interaction of our model would certainly favor saturation, although it need not be its sole cause. The exchange nature of the two-body interactions is known to enter the saturation problem also.

Recently, Brown and co-workers[17,18] have explored the question of three- and four-body forces from a meson-theory viewpoint. In particular, they conclude that the effective mass of a virtual meson is essentially unchanged by intermediate collisions with nucleons and/or other virtual mesons. Our model has no direct meson-meson interaction, but predicts the effective meson mass due to meson-nuclear interactions to be given by Eq. (10). The ground-state instability problem unfortunately invalidates this expression for a coupling constant value of $\lambda^2=5$ that is necessary to give the correct dipole state energy[10] in nuclear matter. Thus, our model is as yet too simple to permit a quantitative comparison with the results of Refs. 17 and 18.

[15] If the calculation of $1/\tau$ according to Eq. (15) with ϵ_{RPA} given by Eq. (5) is continued up to very high momenta $p\sim 2m$ where m is the nucleon mass, a large peak in $1/\tau$ develops. This is brought about by the pole in $D_k(\omega_{pk}^0)=(\omega_{pk}^{02}-\Omega_k^2)^{-1}$. However, this pole and the associated peak are completely spurious. The trouble develops because the nonrelativistic kinematics that is employed in Eq. (5) for the nucleon motion is not valid near $p=2m$. A relativistic treatment of the problem removes the spurious pole.

[16] R. Bryan and B. L. Scott, Phys. Rev. **135**, B434 (1964).

[17] G. E. Brown, A. M. Green, W. J. Gerace, and E. M. Nyman, Nucl. Phys. **A118**, 1 (1968).

[18] G. E. Brown, A. M. Green, and W. J. Gerace, Nucl. Phys. **A115**, 435 (1968).

ACKNOWLEDGMENTS

We would like to thank Gerrie Grosskopf and members of the IBM 360 computer facility at the South African Atomic Energy Board for invaluable assistance in carrying out the numerical computations reported in this paper. Many conversations with Dr. C. A. Engelbrecht are also gratefully acknowledged. One of us (CBD) would like to thank Dr. S. J. du Toit, Director of the Physics Division of the Atomic Energy Board, the Atomic Energy Board, and the University of South Africa for travel support and the hospitality he enjoyed at both these institutions.

APPENDIX A: SOME PROPERTIES OF FUNCTIONS $\pi_0(k,\omega)$

The function $\Pi_0(k,\omega)$ is defined in Eq. (4) of the text for real values of ω. In our applications, we require the function $\Pi_0(k,\omega+i\eta)$, where η is a positive infinitesimal. This function may be written as

$$\Pi_0(k,\omega+i\eta) = \sum_{|\mathbf{p}+\mathbf{k}|>p_F>p} [(\omega^0_{pk}-\omega-i\eta)^{-1}+(\omega^0_{pk}+\omega+i\eta)^{-1}]. \quad \text{(A1)}$$

Both the real and imaginary parts of $\Pi_0(k,\omega+i\eta)$ are obtainable in closed form from this expression. We have

$$\mathrm{Re}\Pi_0(k,\omega+i\eta) = \sum_{|\mathbf{p}+\mathbf{k}|>p_F>p} \frac{2\omega^0_{pk}}{\omega^{02}_{pk}-\omega^2} = \frac{mp_F}{2\pi^2} B(k,\omega), \quad \text{(A2)}$$

where

$$B(k,\omega) = \tfrac{1}{2} + \frac{p_F}{4k}\left[\left(\frac{\omega+k^2/2m}{kv_F}\right)^2-1\right]\ln\left|\frac{\omega-\omega_<}{\omega+\omega_>}\right| - \frac{p_F}{4k}\left[\left(\frac{\omega-k^2/2m}{kv_F}\right)^2-1\right]\ln\left|\frac{\omega-\omega_>}{\omega+\omega_<}\right|. \quad \text{(A3)}$$

Here, $v_F=p_F/m$ is the velocity of a particle at the Fermi surface, and $\omega_<=kv_F-k^2/2m$, $\omega_>=kv_F+k^2/2m$, the latter energy representing the maximum particle-hole energy for fixed k. The imaginary part also follows from Eq. (A1) on letting η approach zero. For positive ω only the first term in the bracket contributes, and

$$\mathrm{Im}\Pi_0(k,\omega+i\eta) = \pi \sum_{|\mathbf{p}+\mathbf{k}|>p_F>p} \delta(\omega-\omega^0_{pk}) = \pi S_0(k,\omega), \quad \text{(A4)}$$

where $S_0(k,\omega)$ is the so-called dynamic form factor for the noninteracting Fermi system. Expressions for $S_0(k,\omega)$ are given, for example, in Ref. 4. We specialize

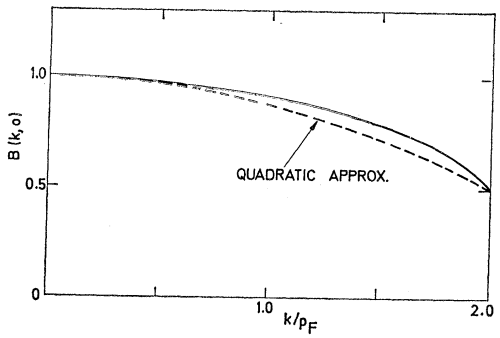

FIG. 3. The function $B(k, 0)$ given by Eq. (A6) (solid curve) compared with the quadratic approximation, Eq. (A7) (dashed curve).

those expressions to our case to find

$$S_0(k,\omega)=\left(\frac{1}{2\pi}\right)^2\frac{m^2\omega}{k}, \qquad 0<\omega<\omega_< \quad \text{and} \quad k<2p_F$$

$$=\left(\frac{1}{2\pi}\right)^2\frac{mp_F^2}{2k}\left[1-\left(\frac{\omega}{kv_F}-\frac{k}{2p_F}\right)^2\right],$$

$$|\omega_<^F|<\omega<\omega_>$$

$$=0 \qquad \text{otherwise.} \tag{A5}$$

The function $B(k, \omega)$ has the exact value

$$B(k,0)=\tfrac{1}{2}+(1/4x)(1-x^2)\ln|(1+x)/(1-x)|, \qquad x=k/2p_F \tag{A6}$$

at $\omega=0$. Migdal[19] notes that $B(k, 0)$ can be adequately represented in the interval $0\leq x\leq 1$ by

$$B(k,0)\approx 1-\tfrac{1}{2}x^2=1-\tfrac{1}{8}(k/p_F)^2. \tag{A7}$$

This expression was used to obtain Eq. (8) in the text. The quality of the validity of (A7) is shown in Fig. 3 by comparing it with the exact expression (A6) for $B(k, 0)$.

Furthermore, $B(k, \omega)$ possesses the useful expansions

$$B(k,\omega)\approx B(k,0)[1-(\omega/\omega_<)(\omega/\omega_>)], \qquad \omega\ll|\omega_<|<\omega_> \tag{A8}$$

and

$$B(k,\omega)\approx 1+(\omega/2\omega_k)\ln|(\omega-\omega_k)/(\omega+\omega_k)|, \qquad \omega_k=kv_F, \quad k\ll 2p_F \tag{A9}$$

that hold, respectively, for small frequencies but any k and small momenta but any frequency.

Two further useful forms of Eq. (A9) are available if ω and ω_k are very different:

$$B(k,\omega)\approx 1-(\omega/\omega_k)^2, \qquad \omega\ll\omega_k \tag{A10}$$

and

$$B(k,\omega)\approx -\tfrac{1}{3}(\omega_k/\omega)^2, \qquad \omega\gg\omega_k. \tag{A11}$$

[19] A. Migdal, Zh. Eksperim. i Teor. Fiz. **34**, 1438 (1958) [English transl.: Soviet Phys.—JETP **7**, 996 (1958)].

The latter expression leads directly to the result quoted as Eq. (12), for

$$g\Pi_0(k,\omega)\approx g(mp_F/2\pi^2)(-\tfrac{1}{3})(kv_F/\omega)^2=-N(k^2/m\omega^2), \tag{A12}$$

since $gp_F^3/6\pi^2$ is the particle density of a Fermi system with momentum p_F.

APPENDIX B: ANALYTICITY PROPERTIES OF $\epsilon_{\mathrm{RPA}}(k, \omega)$

The causal dielectric constant[20] is given by Eq. (5) of the text using the definition (A1) for $\Pi_0(k, \omega)$:

$$\epsilon_{\mathrm{RPA}}(k,\omega+i\eta)=1+g\lambda^2D_k(\omega)\Pi_0(k,\omega+i\eta). \tag{B1}$$

The attachment of $i\eta$ to ω causes the function $\epsilon_{\mathrm{RPA}}^{-1}$ to be analytic in the entire upper half ω plane.[7] This fact is made use of in obtaining the formula (15) of Quinn and Ferrell quoted in the text. It can be shown further that ϵ_{RPA} is also analytic in the upper half ω plane provided that[7]

$$\epsilon_{\mathrm{RPA}}(k,0)>0 \qquad \text{for all } k. \tag{B2}$$

For the electron gas system, this condition is related to the stability of the system against a background of positive neutralizing charge.[7] It is interesting to see that the condition (B2) relates to the stability of the ground state of the nuclear matter system. To see this note that

$$\epsilon_{\mathrm{RPA}}(k,0)=1-\frac{\lambda^2}{\lambda_c^2}\frac{B(k,0)}{(1+k^2/\mu^2)}, \tag{B3}$$

where λ_c is the critical coupling constant defined by Eq. (11) in the text. Now observe that the ratio $B(k, 0)/(1+k^2/\mu^2)$ is a monotonically decreasing function as k increases, so that (B2) will be satisfied for all k if it is satisfied at $k=0$, i.e., if

$$\epsilon_{\mathrm{RPA}}(0,0)=1-(\lambda^2/\lambda_c^2)B(0,0)>0. \tag{B4}$$

Since $B(0, 0)=1$, this means that the condition (B2) is satisfied for all coupling constants below the critical value λ_c. For $\lambda>\lambda_c$, the ground-state stability and the analyticity of ϵ_{RPA} are violated simultaneously; one might think of the system as "over reacting" to an external applied applied field in this case and acquiring a permanent density fluctuation in the ground state in the process.

APPENDIX C: EXPLICIT FORMULAS FOR INVERSE QUASIPARTICLE LIFETIME

(a) For the dressed interaction, we replace $\mathbf{k}$ by $-\mathbf{k}$ in Eq. (18) of the text and go over from a sum to an

[20] The analogous expression to (B1) for ϵ_{RPA} for an electron gas is given for example in Ref. 7. We take this opportunity to correct a misprint of an over-all factor of $\frac{1}{2}$ that is missing from the center expression in Eq. (5.63), p. 287 of that reference.

integral by the usual replacement $\sum_k \to (2\pi)^{-3}\int d\mathbf{k}$. Then

$$\tau^{-1}=\frac{2}{(2\pi)^2}\int_0^{2p}k^2dk\int' d(\cos\theta_{pk})\left\{\frac{[\lambda^2D_k(\omega)][\pi g\lambda^2D_k(\omega)S_0(k,\omega)]}{[1+g\lambda^2D_k(\omega)(mp_F/2\pi^2)B(k,\omega)]^2+[\pi g\lambda^2D_k(\omega)S_0(k,\omega)]^2}\right\}_{\omega=\epsilon_p-\epsilon_{p-k}}. \quad \text{(C1)}$$

Here, θ_{pk} represents the angle between the variable vector $\mathbf{k}$ and the fixed vector $\mathbf{p}$ that serves as a polar axis for the integration over $\mathbf{k}$. The restrictions on k and the variable $\cos\theta_{pk}$ (indicated by the prime on the second integral sign) are best appreciated by looking at Fig. 4. Since [Eq. (16) with $\mathbf{k}=-\mathbf{k}$]

$$p^2 > |\mathbf{p}+\mathbf{k}|^2 > p_F^2, \quad \text{(C2)}$$

the extremity of the vector $\mathbf{k}$ must always lie in the region between two spheres of radii p_F and p that share a common origin. The length of $\mathbf{k}$ varies between 0 and $2p$. However, the limits on $\cos\theta_{pk}$ depend on the value of k, varying from $-k/(2p)$ to either $-(p^2-p_F^2-k^2)/2pk$ if $p-p_F<k<p+p_F$, or -1 if $0<k<p-p_F$.

Introducing the dimensionless variables

$$x=\cos\theta_{pk}; \quad y=p/p_F; \quad z=k/p_F;$$
$$\alpha=\mu/p_F; \quad \beta=p_F/2m; \quad \gamma=g\lambda^2/16\pi\beta, \quad \text{(C3)}$$

the expression for $1/\tau$ becomes

$$\tau^{-1}=\frac{\lambda^2p_F}{2\pi^2}\int_0^{2y}z^2dz\int_{\max\{(1-y^2-z^2)/2yz,-1\}}^{-z/2y}dx\,C(x,y,z)$$
$$\times\left\{\left[\beta^2z^2(z+2xy)^2-\alpha^2-z^2+\frac{4\gamma}{\pi}B(x,y,z)\right]^2+C^2(x,y,z)\right\}^{-1}, \quad \text{(C4)}$$

where the limits are now explicit. The functions B and C are

$$B(x,y,z)=\tfrac{1}{2}+(4z)^{-1}(x^2y^2-1)\ln\left|\frac{1+xy}{1-xy}\right|$$
$$-(4z)^{-1}[(z+xy)^2-1]\ln\left|\frac{1+xy+z}{1-xy-z}\right|,$$

$$C(x,y,z)=\pi(g\lambda^2/p_F^2)S_0(k,\epsilon_p-\epsilon_{p+k}).$$

Using Eq. (A5), the function C has two forms depending on whether z is less than or greater than 2. For $z<2$

$$C(x,y,z)$$
$$=(\gamma/z)[1-(z+xy)^2] \quad \text{if} \quad -(1+z)/y\le x\le -1/y$$
$$=-\gamma(z+2xy) \quad \text{if} \quad -1/y\le x\le -z/2y$$
$$=0 \quad \text{otherwise,}$$

while for $z>2$

$$C(x,y,z)$$
$$=(\gamma/z)[1-(z+xy)^2] \quad \text{if} \quad -(1+z)/y\le x\le (1-z)/y$$
$$=0 \quad \text{otherwise.}$$

Equation (C4) was integrated numerically to obtain the results shown in Fig. 2 of the text. The dressed static interaction case [corresponding to using $D_k(0)$ in Eq. (C1)] is obtained upon suppression of the factor $\beta^2z^2(z+2xy)^2$ in the denominator of Eq. (C4).

(b) For the bare interaction (static), we obtain $1/\tau$ by setting the denominator in Eq. (C1) equal to unity and using $D_k(0)$ in place of $D_k(\omega)$. Thus,

$$\left(\frac{1}{\tau}\right)_{\text{bare}}=\frac{\pi g\lambda^4}{2\pi^2}\int_0^{2p}dk\,k^2D_k^2(0)$$
$$\times\int' d(\cos\theta_{pk})S_0(k,\epsilon_p-\epsilon_{p+k}). \quad \text{(C5)}$$

The integration over $\cos\theta_{pk}$ is best performed by shifting to the variable[7,12]

$$\omega'=\epsilon_p-\epsilon_{p+k}=-[k^2/2m+(pk/m)\cos\theta_{pk}],$$

from which it follows that $d(\cos\theta_{pk})=-(m/pk)d\omega'$. The angular integral then reads

$$\frac{m}{pk}\int_0^{\omega'_{\max}}d\omega'S_0(k,\omega'). \quad \text{(C6)}$$

The value of $\omega'_{\max}$ again depends on k: Looking back at Fig. 4, we find

$$\omega'_{\max}=(pk/m)-(k^2/2m) \quad \text{if} \quad 0<k<p-p_F$$
$$=\epsilon_p-\epsilon_F \quad \text{if} \quad p-p_F<k<p+p_F. \quad \text{(C7)}$$

If $k>p+p_F$, the resulting value of $\omega'_{\max}$ exceeds the

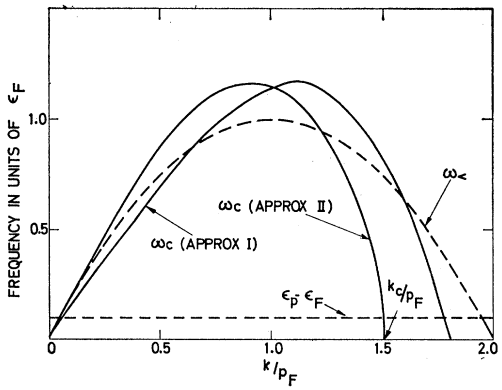

FIG. 4. The function $\omega_c(k)$ as given by approximation II, Eq. (D4), and approximation I, Eq. (D5). The dashed curve gives the upper limit to the exact function $\omega_c(k)$. The cutoff wave number k_c and a typical value of $\epsilon_p-\epsilon_F$ that is considered in the derivation of Eqs. (D9) and (D10) are indicated.

maximum particle-hole energy $\omega_>$ and $S_0(k,\omega')$ vanishes accordingly. Therefore, we may write

$$\omega'_{\max}=\omega'_{\max}(k)=\min\{\epsilon_p-\epsilon_F, kp/m-k^2/2m\} \quad \text{(C8)}$$

for the upper limit in Eq. (C6).

The region of integration covered in Eq. (C6) depends on p and k. Since $S_0(k,\omega')$ has a different functional form depending on where ω' lies, the conditions on ω' in (A5) are superposed on the conditions (C8), and so one finds that the integral (C5) has a different functional form in the three regimes (i) $p_F<p<\sqrt{2}p_F$, (ii) $\sqrt{2}p_F<p<3p_F$, and (iii) $3p_F<p$ of the momentum p. We write

$$\left(\frac{1}{\tau}\right)_{\text{bare}}=m\frac{g\lambda^4}{16\pi^3}\frac{p_F}{p}I\left(\frac{p}{p_F}\right). \quad \text{(C9)}$$

The function $I(p/p_F)$ is given by the following forms (measuring p and μ in units of p_F):

(i) $1<p<\sqrt{2}$, $I=I_1(p)$. Define $p_<=1-(2-p^2)^{1/2}$ and $p_>=1+(2-p^2)^{1/2}$. Then,

$$\begin{aligned}
I_1(p)=&-\tfrac{1}{12}p_<-\frac{1}{2}\frac{(1+\frac{1}{12}\mu^2)(p-1)}{\mu^2+(p-1)^2}+\frac{1}{8}\frac{(p^2-1)^2}{\mu^2}\left[\frac{p_>}{\mu^2+p_>^2}-\frac{p_<}{\mu^2+p_<^2}\right]+\frac{1}{24}\frac{(p^2-1)^3}{\mu^4}\\
&\times\left[\frac{1}{p_<}-\frac{1}{p_>}+\frac{1}{p+1}-\frac{1}{p-1}\right]+\frac{1}{3}\left[\frac{2}{\mu^2+4}+\frac{1}{\mu^2+p_<^2}-\frac{1}{\mu^2+p_>^2}-\frac{1}{\mu^2+(p-1)^2}-\frac{1}{\mu^2+(p+1)^2}\right]\\
&+\frac{1}{16}\left[\frac{p+1}{\mu^2+(p+1)^2}-\frac{2}{\mu^2+4}\right]\left[\frac{1}{3}\frac{(p^2-1)^3}{\mu^4}+\frac{(p^2-1)(p^2+3)}{\mu^2}+p^2+3+\tfrac{1}{3}\mu^2\right]\\
&+\frac{1}{16}\left[\frac{2}{\mu^2+4}+\frac{p_<}{\mu^2+p_<^2}-\frac{p_>}{\mu^2+p_>^2}-\frac{(p-1)}{\mu^2+(p-1)^2}\right]\left[\frac{1}{3}\frac{(p^2-1)^3}{\mu^4}+\frac{(p^2-1)(p^2+3)}{\mu^2}-5+p^2-\tfrac{1}{3}\mu^2\right]\\
&+\frac{1}{8}\frac{\mu^2+4}{\mu}\tan^{-1}\left(\frac{p-1}{\mu}\right)+\frac{1}{8}\frac{(p^2-1)^2}{\mu^3}\left[\tan^{-1}\left(\frac{p_>}{\mu}\right)-\tan^{-1}\left(\frac{p_<}{\mu}\right)\right]+\frac{1}{16}\left[\frac{(p^2-1)^3}{\mu^5}+\frac{(p^2-1)(p^2+3)}{\mu^3}-\frac{p^2+3}{\mu}-\mu\right]\\
&\times\left[\tan^{-1}\left(\frac{p+1}{\mu}\right)-\tan^{-1}\left(\frac{2}{\mu}\right)\right]+\frac{1}{16}\left[\frac{(p^2-1)^3}{\mu^5}+\frac{(p^2-1)(p^2+3)}{\mu^3}+\frac{5-p^2}{\mu}+\mu\right]\\
&\times\left[\tan^{-1}\left(\frac{p_<}{\mu}\right)-\tan^{-1}\left(\frac{p_>}{\mu}\right)+\tan^{-1}\left(\frac{2}{\mu}\right)-\tan^{-1}\left(\frac{p-1}{\mu}\right)\right].
\end{aligned}$$

(ii) $\sqrt{2}<p<3$. Let $I=I_2(p)$. Then,

$$\begin{aligned}
I_2(p)=&I_1(p)-\tfrac{1}{24}(p_>-p_<)-\frac{1}{24}\frac{(p^2-1)^3}{\mu^4}\left(\frac{1}{p_<}-\frac{1}{p_>}\right)-\frac{1}{3}\left(\frac{1}{\mu^2+p_<^2}-\frac{1}{\mu^2+p_>^2}\right)\\
&-\frac{1}{16}\left[\frac{p_<}{\mu^2+p_<^2}-\frac{p_>}{\mu^2+p_>^2}\right]\left[\frac{1}{3}\frac{(p^2-1)^3}{\mu^4}+\frac{(5-p^2)(p^2-1-\mu^2)}{\mu^2}-\tfrac{1}{3}\mu^2\right]\\
&-\frac{1}{16}\left[\tan^{-1}\left(\frac{p_<}{\mu}\right)-\tan^{-1}\left(\frac{p_>}{\mu}\right)\right]\left[\frac{(p^2-1)^3}{\mu^5}+\frac{(5-p^2)(p^2-1+\mu^2)}{\mu^3}+\mu\right].
\end{aligned}$$

Finally, (iii) $3<p$, $I=I_3(p)$, where

$$\begin{aligned}
I_3(p)=&-\frac{1}{6}-\frac{1}{3}\left[\frac{1}{\mu^2+(p+1)^2}+\frac{1}{\mu^2+(p-1)^2}\right]-\frac{1}{12}\frac{(p^2-1)^2}{\mu^4}\\
&+\frac{1}{16}\left[\frac{p+1}{\mu^2+(p+1)^2}-\frac{p-1}{\mu^2+(p-1)^2}\right]\left[\frac{1}{3}\frac{(p^2-1)^3}{\mu^4}+\frac{(p^2+3)(p^2-1+\mu^2)}{\mu^2}+\tfrac{1}{3}\mu^2\right]\\
&+\frac{1}{16}\left[\tan^{-1}\left(\frac{p+1}{\mu}\right)-\tan^{-1}\left(\frac{p-1}{\mu}\right)\right]\left[\frac{(p^2-1)^3}{\mu^5}+\frac{(p^2+3)(p^2-1-\mu^2)}{\mu^3}-\mu\right]+\frac{1}{8}\left(\frac{\mu^2+4}{\mu}\right)\tan^{-1}\left(\frac{2}{\mu}\right).
\end{aligned}$$

A test for the correctness of these expressions is provided by the fact that they join smoothly at $p=\sqrt{2}$ and $p=3$. Equation (C9) with the appropriate form of $I(p)$ was used to calculate the uppermost curve in Fig. 2.

APPENDIX D: EFFECT OF AN INSTABILITY IN GROUND STATE ON QUASIPARTICLE LIFETIME

We return to Eq. (C1) of Appendix C and evaluate $1/\tau$ near the Fermi surface. As in Eq. (C6), we transform the integration on $\cos\theta_{pk}$ to one on the variable ω' introduced there. If $p\sim p_F$ the upper limit on ω' is always the (small) frequency $\epsilon_p-\epsilon_F$ [see Eq. (C7)], and so one has

$$\tau^{-1}\approx\frac{m\lambda^2}{2\pi^2 p_F}\int_0^{2p_F}kdk\int_0^{\epsilon_p-\epsilon_F}d\omega'\,\frac{\pi g\lambda^2 S_0(k,\omega')}{[D_k^{-1}(\omega')+g\lambda^2(mp_F/2\pi^2)B(k,\omega')]^2+[\pi g\lambda^2 S_0(k,\omega')]^2}. \tag{D1}$$

The ω' integration may now be performed by evaluating the integrand at some average value $\bar\omega$ lying in the interval $0<\bar\omega<\epsilon_p-\epsilon_F$ and multiplying by $\epsilon_p-\epsilon_F$. Thus,

$$\tau^{-1}\approx\frac{m\lambda^2}{2\pi^2 p_F}(\epsilon_p-\epsilon_F)\int_0^{2p_F}kdk\,\frac{\pi g\lambda^2 S_0(k,\bar\omega)}{[D_k^{-1}(\bar\omega)+g\lambda^2(mp_F/2\pi^2)B(k,\bar\omega)]^2+[\pi g\lambda^2 S_0(k,\bar\omega)]^2} \tag{D2}$$

approximately. Since $S_0(k,\bar\omega)\sim\bar\omega\sim\epsilon_p-\epsilon_F$, this equation ordinarily leads to the usual result that $1/\tau\sim(\epsilon_p-\epsilon_F)^2$ or $\sim(p-p_F)^2$ for p near p_F. However, this conclusion is invalidated if the ground state is unstable with respect to a permanent density fluctuation, as we now proceed to demonstrate. The point is that such an instability is always accompanied by a zero[1] of

$$D_k^{-1}(\omega)+g\lambda^2(mp_F/2\pi^2)B(k,\omega) \tag{D3}$$

at $\omega=\omega_c(k)$, say. The "instability root" $\omega_c(k)$ always lies below the frequency $\omega_<=kv_F-k^2/2m$ in any event.[1] However, our interest is in regions of k where $\omega_c(k)\sim\bar\omega$, i.e., where $\omega_c(k)$ is a very small frequency. Then Eq. (A8) can be used to obtain a qualitative idea of how $\omega_c(k)$ depends on k in such regions. Combining (D3) and (A8), one finds

$$\omega_c(k)\approx(\omega_<\omega_>)^{1/2}\left[1-\alpha^2\frac{1+k^2/\mu^2}{B(k,0)}\right]^{1/2}$$

$$\approx(\omega_<\omega_>)^{1/2}\left[1-\alpha^2\frac{1+k^2/\mu^2}{1-\frac{1}{8}(k^2/p_F^2)}\right]^{1/2}, \tag{D4}$$

the latter form making use of the approximation (A7) for $B(k,0)$. The function (D4) is shown in Fig. 4 labeled as approximation II. Comparison with the exact upper bound $\omega_<$ (dashed curve) shows that Eq. (D4) is a tolerable approximation for $k\gtrsim1.4p_F$ up to a cutoff frequency

$$k_c=\mu\left\{\frac{(1-\alpha^2)}{(\mu^2/8p_F^2+\alpha^2)}\right\}^{1/2}\approx1.5p_F$$

[set $g\lambda^2=20$ and calculate $g\lambda_c^2=1.42$ from Eq. (11), so that $\alpha=0.071$]. Since $\omega_c(k)\sim\omega_<$ near $k=0$, Eq. (D4) is numerically unreliable for small wave numbers. However, the qualitative conclusion $\omega_c(k)\sim kv_F$ that it leads to is correct as we now show. Since small wave numbers are at issue, we use the approximation (A9) for $B(k,\omega)$ instead in Eq. (D3) to find that

$$\omega_c(k)\approx kv_F\tanh[1-\alpha^2(1+k^2/\mu^2)] \tag{D5}$$

or $\omega_c(k)=0.73kv_F$ near $k=0$, if $\alpha=0.071$. Therefore, approximation II is still qualitatively correct near $k=0$. The function (D5) is also shown in Fig. 4 as approximation I. It is of course only numerically reliable for $k\ll2p_F$.

Figure 4 shows that if the energy difference $\epsilon_p-\epsilon_F<\omega_<$, both zeros of $\omega_c(k)=\epsilon_p-\epsilon_F$ occur in the integration over in Eq. (D2). To see what effect this has, rewrite Eq. (D2) in the form

$$1/\tau=(\lambda^2m/2\pi^2p_F)(\epsilon_p-\epsilon_F)\times\text{integral}, \tag{D6}$$

where

$$\text{integral}=\int_0^{2p_F}kdk\,\frac{\pi g\lambda^2 S_0(k,\bar\omega)}{\xi^2[\bar\omega^2-\omega_c^2(k)]^2+[\pi g\lambda^2 S_0(k,\bar\omega)]^2}, \tag{D7}$$

using the abbreviation $\xi=\mu^2B(k,0)/\alpha^2\omega_<\omega_>$. We now proceed to show that this integral is approximately constant instead of varying like $\epsilon_p-\epsilon_F$, if the system possesses an instability. The main contributions to this integral come from values of k where $\omega_c(k)=\bar\omega$, which, for small $\bar\omega\sim\epsilon_p-\epsilon_F$ are either $k\sim0$ or $k\sim k_c$. Let us obtain the contribution from the region around k_c first. To this end, expand as follows:

$$\bar\omega^2-\bar\omega_c(k)^2\approx-(k^2-k_c^2)(\partial\omega_c^2/\partial k^2)_{k_c}=(1/\xi)(k^2-k_c^2).$$

The last step follows after using Eq. (D4) for $\omega_c^2(k)$. Hence, the integral in (D7) becomes

$$\int_0^{2p_F}kdk\,\frac{\pi g\lambda^2 S_0(k,\bar\omega)}{(k^2-k_c^2)^2+[\pi g\lambda^2 S_0(k,\bar\omega)]^2}\approx\tfrac{1}{2}\pi, \tag{D8}$$

if the integration is performed approximately by allowing k to range from $-\infty$ to $+\infty$. This is permissible, since the integrand in (D8) is a Lorentzian (in k^2 space) with a half-width

$$\gamma_c^2=2\pi g\lambda^2 S_0(k_c,\bar\omega)=g\lambda^2\frac{m^2}{2\pi}\frac{\bar\omega}{k_c}\approx g\lambda^2\frac{mp_F}{2\pi}\left(\frac{p-p_F}{k_c}\right). \tag{D9}$$

This is much smaller than the integration interval $4p_F^2(\gamma_c^2/4p_F^2\sim10^{-2})$ because of the controlling factor $(p-p_F)/k_c$. The width at the other root of $\bar\omega=\omega_c(k)$ near $k=0$ is, by contrast, of the order of the interval of

integration,

$$\gamma_0^2 \approx g\lambda^2(mp_F/2\pi) \sim 4p_F^2, \qquad \text{(D10)}$$

since $\omega_c(k)/k \sim v_F$ is independent of k in this limit. Therefore, only the region around $k=k_c$ contributes significantly giving a factor $\frac{1}{2}\pi$ according to (D8), so that

$$1/\tau \approx (\lambda^2 m/2\pi^2 p_F)(\epsilon_p - \epsilon_F)\tfrac{1}{2}\pi = (\lambda^2/4\pi)(p-p_F), \quad \text{or} \quad 113(p/p_F-1)\ \text{MeV}. \qquad \text{(D11)}$$

The above estimate compares favorably with the value $144(p/p_F-1)$ MeV obtained by numerical integration of Eq. (C1) near $p=p_F$. This agreement indicates that the interpretation of the origin of the unphysical $p-p_F$ behavior of $1/\tau$ near the Fermi surface is indeed correct.

As $\epsilon_p-\epsilon_F$ increases, Fig. 4 suggests that the ratio $\bar{\omega}/k$ increases; the widths γ^2 grow and the instability becomes less important, until at $\epsilon_p-\epsilon_F=(\omega_<)_{\max}=\epsilon_F$ or $p=\sqrt{2}p_F$, when the equation $\bar{\omega}=\omega_c(k)$ certainly has no real roots any more, and the effect of the instability becomes negligible.

Finally, we remark that variational treatments of the unstable ground state have been devised[21] that remove the instability. What role, if any, the root $\omega_c(k)$ has when this is the case has not been investigated yet.

[21] K. Sawada and N. Fukuda, Progr. Theoret. Phys. (Kyoto) **25**, 653 (1961); C. B. Dover, Ph.D. thesis, Massachusetts Institute of Technology, 1967 (unpublished).

PHYSICAL REVIEW VOLUME 183, NUMBER 4 20 JULY 1969

Gamma-Ray Widths in C^{13}, Li^6, and P^{31}

V. K. RASMUSSEN AND C. P. SWANN
Bartol Research Foundation of The Franklin Institute, Swarthmore, Pennsylvania 19081

(Received 24 February 1969)

The width of the 3.68-MeV level of C^{13} has been measured and found to be $\Gamma=0.44\pm0.04$ eV. After correction for the E^3 dependence, this is 0.59 times as strong as the mirror transition in N^{13}, in agreement with Morpurgo's prediction of approximate equality for $M1$, $\Delta T=0$ transitions in mirror nuclei. The C^{13} width was obtained from a comparison of the resonant scattering of bremsstrahlung by C^{13} with that by the 3.51-MeV level of P^{31} and the 3.56-MeV level of Li^6. The widths of the P^{31} and Li^6 levels were measured in self-absorption experiments, and found to be 52 ± 8 meV and 8.1 ± 0.5 eV, respectively. A limit on the energetically allowed but spin- and parity-forbidden decay of the Li^6 level to $\alpha+d$ was established as $\Gamma_{\alpha d}<1.3$ eV.

INTRODUCTION

THE rules of Morpurgo concerning the relative strengths of γ transitions between corresponding states of mirror nuclei follow directly from charge independence or charge symmetry,[1,2] principles so well established on other grounds that the rules seem to be referred to most frequently when used as an aid in correlating mirror levels, with no great experimental effort being devoted to their verification. It would seem, however, that any experimental results might challenge the theorists to construct more accurate and detailed wave functions. We have previously shown,[3] for example, that corresponding $E1$ transitions in C^{13} and N^{13}, which should be equal, according to Morpurpo's predictions, differ by a factor of 2. This difference is qualitatively understandable, but would seem to be worthy of a more detailed study. Warburton *et al.*[4] discuss a similar case in N^{15}-O^{15}.

The subject of the present paper is an $M1$ ($\Delta T=0$) transition in the C^{13}-N^{13} pair. Here Morpurgo has shown one can deduce both the isospin-independent and the isospin-dependent parts of the matrix element from comparison with experiment.

Our measurements are concerned primarily with using resonance-fluorescence techniques to measure the width of the 3.68-MeV level of C^{13}. Since samples of C^{13} large enough for a self-absorption measurement are not easily available, the scattering was compared with scattering by the 3.56-MeV level of Li^6 and the 3.51-MeV level of P^{31}, for which accurate widths could be established by self-absorption measurements.

EXPERIMENTAL DETAILS

The photon beam for our resonance fluorescence measurements is produced when the electron beam

[1] G. Morpurgo, Phys. Rev. **114**, 1075 (1959).
[2] W. M. McDonald, in *Nuclear Spectroscopy, Part B*, edited by F. Ajzenberg-Selove (Academic Press Inc., New York, 1960).
[3] S. W. Robinson, C. P. Swann, and V. K. Rasmussen, Phys. Letters **26B**, 298 (1968).
[4] E. K. Warburton, J. W. Olness, and D. E. Alburger, Phys. Rev. **140**, B1202 (1965).